Characterization of Rat NTPDase1, -2, and -3 Ectodomains Refolded from Bacterial Inclusion Bodies†

Matthias Zebisch and Norbert Sträter*

Center for Biotechnology and Biomedicine, Institute of Bioanalytical Chemistry, Faculty of Chemistry and Mineralogy, University of Leipzig, Deutscher Platz 5, 04103 Leipzig, Germany

Received June 19, 2007; Revised Manuscript Received August 9, 2007

ABSTRACT: The ecto-nucleoside triphosphate diphosphohydrolases or NTPDases are a family of membrane-bound enzymes that catalyze the sequential removal of γ- and β-phosphate from ATP, ADP, and other nucleotides. NTPDase1, -2, -3, and -8 are the enzymes responsible for signal conversion and termination in purinergic signaling. They are anchored to the cytoplasmic membrane by two transmembrane helices with a large catalytic domain pointing toward the extracellular space. Here we report the first successful expression and purification of the soluble extracellular domains of rat NTPDase1, -2, and -3 from bacterial inclusion bodies. The refolded proteins show characteristics similar to the wild type enzymes, for example in that they are dependent on divalent metal ions for catalysis and hydrolyze a wide variety of nucleoside tri- and diphosphates, whereas the monophosphate AMP is not further degraded. Nucleoside triphosphates are hydrolyzed at a higher rate than the corresponding diphosphates. Other characteristics of the recombinant enzymes however reflect the absence of transmembrane regions and side chain glycosylation. For example all three enzymes are monomeric and only subtly activated by Mg^{2+} ions as compared to Ca^{2+} ions. Although having a considerably higher specificity constant k_{cat}/K_m for ADP as for ATP, the bacterially expressed variant of NTPDase1 in contrast to its wild type counterpart releases intermediate ADP to a substantial amount. The presented expression system will allow large scale production of active protein suitable for structural studies, development of inhibitors, and even clinical application.

ATP when released from cells acts extracellularly as a signaling molecule in an autocrine or paracrine manner (*1*−*3*). Cellular responses are induced through activation of G-protein-coupled P2Y receptors or ligand-gated ion channels (P2X). It is now evident that a cascade of membrane-bound enzymes located on the cell surface modulates and inactivates those signaling effects. The ecto-nucleoside triphosphate diphosphohydrolases1, -2, -3, and -8 (NTPDases, EC 3.6.1.5) are oligomeric enzymes responsible for the first steps of extracellular nucleotide degradation (*4*−*7*). They catalyze the sequential removal of γ- and β-phosphate from triphosphonucleosides to produce the corresponding monophosphonucleoside. AMP is not a substrate for NTPDases; instead it is degraded to adenosine by ecto-5′-nucleotidase (5′NT or CD73) (*4*, *5*). Crystal structures are available for *E. coli* 5′NT, which has an active site structure similar to that of the vertebrate 5′NT (*8*, *9*). 5′NT and the NTPDases are evolutionarily unrelated.

In contrast to the extracellular NTPDases, the closely related NTPDase4−7 are less active toward ATP and ADP and in the case of NTPDase5 and -6 more specifically cleave diphosphonucleosides. They are located intracellularly with their catalytic domain facing the lumen of cytoplasmic organelles such as the Golgi or the endoplasmatic reticulum. It has been suggested that they participate in sugar nucleotide transfer and transport processes (*10*−*12*).

Firmly anchored to the cell membrane by two transmembrane helices, the large catalytic domain of NTPDase1−3 and -8 is exposed to the extracellular milieu (*7*, *13*−*15*). Similar to other extracellular proteins, the ectodomain is stabilized by five invariant disulfide bridges (*16*, *17*) and carries several N-linked oligosaccharide chains (*18*−*22*). The amino acid identity within the catalytic domain of different NTPDases is especially high in five 'apyrase conserved regions' (ACR). ACR1 and -4 exhibit similarity to the β- and γ-phosphate binding motifs of the actin/hsp70/sugar kinase superfamily (*23*). Although no additional significant sequence identity between soluble members of this superfamily and the NTPDase ectodomain exists, their common structural fold could be revealed using comparative analysis of predicted secondary structure and threading studies (*14*, *17*, *24*, *25*). The catalytic ectodomain of NTPDases is thus

† For financial support, funding by the Deutsche Forschungsgemeinschaft and by EFRE funds of the European Union is acknowledged.

* Author to whom correspondence should be addressed. Tel.: +49-(0)341-9731311. Fax: +49-(0)341-9731319. E-mail: strater@bbz.uni-leipzig.de.

[1] Abbreviations: ABD-F, 7-fluoro-2,1,3-benzoxadiazole-4-sulfonamide; ACR, apyrase conserved region; BSA, bovine serum albumin; CHO cell, Chinese-hamster ovary cell; COS cell, African-green-monkey kidney cell; DTT, dithiothreitol; GdmCl, guanidinium chloride; GSSG/GSH oxidized/reduced glutathione; IPTG, isopropyl β-D-thiogalactopyranoside; MOPS, 3-(N-morpholino)propanesulfonic acid; NTPDases, nucleoside triphosphate diphosphohydrolases; PAGE, polyacrylamide gel electrophoresis; P_i, inorganic phosphate; PP_i, inorganic pyrophosphate; PMSF, phenylmethanesulfonyl fluoride; RP-HPLC, reversed phase high performance liquid chromatography; TCA, trichloroacetic acid; TCEP, tris(2-carboxyethyl)phosphine.

10.1021/bi701103y CCC: $37.00
Published on Web 10/02/2007

likely to consist of two lobes with a large active site cleft in between.

Individual family members of mammalian cell surface NTPDases differ in pH dependence, substrate specificity, and product formation (*15*). NTPDase1 hydrolyzes nucleoside diphosphates almost as well as the corresponding triphosphates. The wild type enzyme in its membrane-bound, oligomeric form hydrolyzes ATP directly to AMP through subsequent scission of both phosphoanhydride bonds with almost no release of intermediate ADP (*15*, *26*−*28*). NTPDase2 conversely is a preferential nucleoside triphosphatase and hydrolyzes ADP 10 to 15 times less efficiently than ATP (*15*, *27*, *29*−*31*). NTPDase3 and -8 are described as functional intermediates between NTPDase1 and -2 (*13*, *15*, *32*, *33*).

Because of their involvement in physiological processes such as blood clotting, vascular inflammation, immune reactions, and in certain types of cancer (*7*, *34*−*43*), NTPDases are now considered as potential new drug targets (*44*−*46*) or drugs themselves. The soluble ectodomain of NTPDase1 from mammalian cell culture has been shown to inhibit platelet aggregation *in vitro* and *in vivo* (*47*−*52*). However, production of large quantities of therapeutic proteins from mammalian cell culture is expensive and bears the risk of viral contamination (*53*, *54*). Therefore and for further biochemical and structural characterization, we sought to establish an *E. coli*-based expression system for production of enzymatically active extracellular domains of NTPDase1−3.

The motivation for the expression system described here are the experiments of Kirley's group (*16*, *55*), who could refold the intracellular NTPDase5 and -6 from bacterial inclusion bodies and the finding of Gayle and others that mammalian cell surface NTPDases still display activity when they are expressed without their transmembrane regions (*28*, *30*, *47*, *56*, *57*).

Here we show that all three enzyme ectodomains can be refolded from *E. coli* cytosolic inclusion bodies to active protein with an overall yield of ≈15 mg of pure protein per liter of high cell density batch fermentation medium. The recombinantly expressed enzyme variants were purified and characterized with respect to substrate specificity and affinity, metal cofactor activation, pH dependence, and product formation. The data indicate that the refolded proteins, although showing differences to their wild type counterparts, will be amenable for inhibitor screening, crystallization, and even clinical application; the latter indicated that the refolding conditions can be conferred from the rat enzymes studied in this work to the human orthologs.

EXPERIMENTAL PROCEDURES

Materials. Tri- and diphosphonucleosides as well as adenosine monophosphate were obtained from Sigma-Aldrich (Steinheim/Germany), deoxynucleotides from Fermentas (St. Leon-Rot/Germany). Stock solutions of nucleotides were adjusted to pH 7.0 with concentrated NaOH and the concentration validated using specific extinction coefficients. L-Arginine was from Ajinomoto Omnichem (Louvain-La-Neuve/Belgium), guanidine hydrochloride C-grade from NIGU Chemie (Waldkraiburg/Germany) and glutathione from Applichem (Darmstadt/Germany). All other chemicals were from Sigma-Aldrich.

Cloning of NTPDase1, -2, and -3 Ectodomain. Full length clones encoding the *R. norvegicus* NTPDase1, -2, and -3 genes (*14*, *26*, *58*) were kindly provided by Prof. Herbert Zimmermann (Biocenter of the J. W. Goethe-University, Frankfurt/Germany). Compared to the sequences deposited in GenBank (accession numbers U81295, Y11835, and AJ437217) the NTPDase1 clone showed several variations: L80Q, S216A, V220I, Q227S, and F331I. All deviating residues except for F331I are also found in the mouse orthologue. Residues Q80, A216, and I220 are furthermore highly conserved among cell surface NTPDases. The side chain of I331 is similar to that of leucine, found in NTPDase1 of other species in the corresponding position. Therefore, these variations are most likely due to sequencing errors in the Genbank entry. The full length clone of rat NTPDase2 showed the previously described variations P127L and F128L (*59*).

By multiple protein sequence alignment (*60*), secondary structure prediction (*61*), and hydrophobicity analysis (e.g., TMpred) of several mammalian cell surface NTPDases, residues T38−T477 (NTPDase1), T29−S462 (NTPDase2), and Q44-P485 (NTPDase3) were estimated to belong to the ectodomain. For standard-PCR-based cloning of the ectodomains into the bacterial expression vector pET-45b(+) (Novagen, Madison, WI), the following primer pairs were designed: 5′-agt ccg gat ccc **acc cac aac aaa cca ttg cca ga**-3′ and 5′-g gcc gca agc *tta* **ggt gga gtg agg gag agg cgg g**-3′ (NTPDase1), 5′-agt ccg gat ccc **acc caa gac gtc cgg gag ccg cc**-3′ and 5′-g gcc gca agc *tta* **gct gaa gtg ggt gcc ctt gcg t**-3′ (NTPDase2), and 5′-agt ccg gat ccc **cag atc cac cac cca cag gtt ct**-3′ and 5′-ccg cca caa caa ttg *tta* **cgg cgg ctg tat ggg tag tt**-3′ (NTPDase3). Flanking the regions coding for the ectodomain (bold) 5′ primers all contained a restriction site (underlined) for the endonuclease *Bam*HI. 3′ primers introduced the strong stop codon taa (*italic*) and a *Hind*III (NTPDase1 and 2) or *Mfe*I (NTPDase3) restriction site. PCR products were digested with both endonucleases and ligated into pET-45b(+) cut with the same enzymes. Recombinant plasmids were transformed by electroporation into *E. coli* ER2566 cells (New England Biolabs, Frankfurt/Germany). Positive clones were identified by colony-PCR and confirmed by restriction digest analysis and DNA sequencing (MWG Biotech, Ebersberg/Germany) with T7 promoter and terminator primer and two custom-synthesized internal primers.

Fermentation of Cells Producing NTPDase Ectodomains. For large scale production of recombinant NTPDases, cells were cultivated in 5 L of glucose mineral salt medium in a 13 L labfors fermenter (Infors, Bottmingen/Switzerland). The composition of the medium was the same as used by Horn et al. (*62*) for the main culture with the exception that 30 g/L glucose was used. Prior to sterilization, the pH was adjusted to 6.4 using 25% (v/v) aqueous ammonia. After 100 μg/mL ampicillin was autoclaved, separately autoclaved glucose and $MgSO_4$ were added and the pH was adjusted to 6.8 with 5 M NaOH. A 20 mL starter culture in LB medium containing 100 μg/mL ampicillin was inoculated from a frozen stock culture. After 6 to 8 h, the fermenter was inoculated with 1 to 3 mL of this starter culture and left unattended over night. The pH was maintained at 6.8 by the implemented control unit using 5 M NaOH and 1 M H_3PO_4. Dissolved oxygen was kept constant at 40 ± 5%

relative saturation by automatic adjustment of the inlet flow of pressurized air. An autoclaved 1% suspension of antifoam A (Sigma-Aldrich) was added when necessary. To further suppress foam formation, pure oxygen gas was mixed into the air stream, when the OD_{600} became greater than 10.

Cultures grew exponentially with a growth rate of 0.58 ± 0.01 h^{-1} to an OD_{600} of 10. Production of the recombinant protein was then induced by addition of 1 mM IPTG. Cultivation of the cells was continued for 4 h or until glucose was completely consumed (sudden decrease in oxygen consumption). Cells were harvested by centrifugation, washed once with ice cold 100 mM TrisHCl, 1 mM EDTA, pH 7.0, and frozen at −20 °C.

Inclusion Body Preparation and Prepurification. Inclusion bodies were isolated and washed generally following the protocol of Rudolph et al. (*63*). Frozen cells (100 g) were resuspended in 500 mL of 100 mM TrisHCl, 1 mM EDTA, pH 7.0, at room temperature. Lysozyme (50 mg) was added and the suspension incubated for 30 min at 4 °C. PMSF, $MgCl_2$, and DNase I (Roche, Mannheim/Germany) were added to a final concentration of 0.2 mM, 3 mM, and 10 μg/mL, respectively. Cell disruption was further achieved by two runs through a APV-2000 cell homogenizer (Invensys APV, Albertslund/Denmark) with cooling in between. Inclusion bodies were separated from the soluble fraction by centrifugation at 31 000*g* for 10 min. After resuspension they were extensively washed twice with 500 mM NaCl, 20 mM EDTA, 2% Triton X-100, pH 8.0 and twice with 100 mM TrisHCl, 20 mM EDTA, pH 7.0, prior to freezing at −20 °C.

A minced inclusion body pellet containing approximately 1 g of protein was solubilized in 50 mL 6 M GdmCl, 100 mM TrisHCl, 1 mM DTT, pH 8.0. Insoluble particles were removed by centrifugation at 48 000*g* for 20 min. The supernatant was applied to a 25 mL Ni-Sepharose column (GE Healthcare Biosciences AB, Uppsala/Sweden) equilibrated with solubilization buffer without DTT at a flow rate of 2 mL/min. The column was washed with three column volumes of 30 mM imidazole in solubilization buffer and the protein eluted with 300 mM imidazole. Any stripped off Ni^{2+} ions were removed by complexation with 1 mM EDTA, thereby avoiding oxidative damage caused by metal catalysis. To completely reduce any artificial disulfide bridges, DTT was added to a final concentration of 100 mM and the solution heated to 50 °C for 20 min. The pH was adjusted to <2.0 by addition of 5 M HCl and the solution then dialyzed three times 24 h against ten volumes of 6 M GdmCl, 5 mM HCl. Such prepurified, completely denatured and reduced protein was stored until further usage at −80 °C.

Determination of Protein Concentration. Protein concentration of the soluble fraction of bacterial cell extracts was determined by Bradford assay using bovine serum albumin in cell lysis buffer as a standard. Protein content in solubilized inclusion bodies was measured spectrophotometrically using equation c (mg/mL) = (1.55 × A_{280}) − (0.76 × A_{260}). Ni^{2+} affinity purified protein was analyzed using the specific extinction coefficients as calculated by the ProtParam tool (*64*, Table 4).

Analytical and Preparative Refolding of Recombinant NTPDases. Concentrated, completely denatured and reduced NTPDase was refolded by means of rapid dilution into nondenaturing buffers. Initial optimization of the refolding conditions for each of the three enzymes used only analytical quantities of unfolded protein in the refolding trials. Typically 1.5 mL of refolding buffer of varying composition was added to a 1.5 mL tube and cooled on ice. The protein solution (e.g., 15 μL, 5 mg/mL) was deposited as a droplet onto the inside face of the lid. After careful closing of the tube, it was vigorously agitated for a few seconds on a Vortex-Genie 2T (Scientific Industries, Bohemia, NY) at maximum speed and then incubated at the indicated temperature. As preliminary tests indicated very slow folding kinetics, the specific activity was measured after 7 to 10 days incubation to allow near end-point determinations. All screened refolding buffers were thoroughly degassed or assembled from degassed stock solutions.

For preparative refolding, 150 mg of the denatured protein were adjusted to 3 mg/mL in 6 M GdmCl, 5 mM HCl. A 5 L amount of the corresponding refolding buffer without the components of the oxido-shuffling system was sterile-filtered, degassed, and cooled to ≤4 °C. Preparative refolding batches all contained 0.1 mM PMSF, 1 mM benzamidine, and 1 mM EDTA to avoid microbial growth and proteolytic degradation. Solid glutathione was added and dissolved only shortly before addition of the unfolded protein. After the solution was transferred to a refolding vessel, it was stirred at 850 rpm by a mixing paddle (70 mm × 400 mm) powered by an overhead stirrer (Heidolph Instruments, Schwabach/Germany). Using a syringe, the denatured protein solution was injected within 1 min through a 0.8 mm needle into the refolding buffer. This procedure almost completely circumvented the precipitation of protein and formation of foam. Finally, the refolding solution was incubated at the indicated temperature.

Purification of Refolded NTPDases. For detailed biochemical analysis of the refolded proteins, it was necessary to separate them from remaining contaminants and misfolded, especially aggregated, protein. The hexahistidine tag encoded by the plasmid was not removed in this work. Preparative refolding batches were concentrated 50-fold using a UFP-10-C-6A hollow fiber ultrafiltration cartridge (GE Healthcare, Buckinghamshire/UK) and then dialyzed two times against 50 volumes of 50 mM sodium acetate, 1 mM EDTA, 0.2 mM PMSF, pH 5.0. During dialysis most of the wrongly folded proteins precipitated, while the active enzyme remained in solution. After 15 min centrifugation at 48 000*g*, the supernatant was applied to an equilibrated 1 mL CM Sepharose Fast Flow column (GE Healthcare, Buckinghamshire/UK) at a rate of 1 mL/min. The column was washed with 20 volumes of 50 mM sodium acetate, 1 mM EDTA, pH 5.0. A linear salt gradient from 0 to 2.0 M NaCl over 20 column volumes was applied to elute the protein. Fractions showing the highest specific activity were pooled, diluted 5-fold with 50 mM TrisHCl pH 8.5, and reconcentrated to ≈5 mg/mL. Remaining aggregates and impurities were removed by size exclusion chromatography on a Superdex S200 26/60 pg column with 10 mM TrisHCl, 1 mM EDTA, 0.1 mM PMSF, pH 8.5 as running buffer.

Nucleotidase Activity Assay. If not stated otherwise, recombinant NTPDase enzyme preparations were incubated at 37 °C in 1 mL of 50 mM TrisHCl, 100 mM NaCl, pH 7.4, with 500 μM $CaCl_2$ and 500 μM ATP. The reaction mixture was prewarmed and the reaction started by addition

of enzyme. After 15 s to 30 min, the released phosphate was measured colorimetrically using a modification of the malachite green assay (*65*). Product formation was restricted to 10% orthophosphate compared to the initial nucleotide concentration. A calibration curve made of six points from 0 to 10% orthophosphate with the same buffer composition except for the protein was always measured and treated identically.

pH dependence was analyzed in the presence of 2 mM nucleotide and 500 μM $CaCl_2$ in a long-range buffer system composed of 40 mM glycine, 40 mM acetic acid, and 40 mM MOPS. The ionic strength was kept constant at 156 mM by addition of NaCl.

Native PAGE and Activity Staining. Purified NTPDase proteins were analyzed for microheterogeneity and oligomeric state by nondenaturing gel electrophoresis. Gels (10 cm wide × 7.3 cm high × 0.75 mm thick) consisted of a 5% stacking gel (125 mM TrisHCl pH 7.5) and a 10% separation gel (375 mM TrisHCl pH 9.0). The running buffer (250 mM Tris/glycine pH 9.0) was precooled to 4 °C. Proteins were separated in a cold room within 3 h using a constant current of 15 mA. When the voltage reached 150 V, it was kept constant at that level for the remaining time to avoid excessive heating. The gel was immersed in 20 mL of 200 mM Tris/glycine pH 8.4 with 10 mM $CaCl_2$ and 10 mM ATP. After 10 min to 1 h incubation at room-temperature, white lines of calcium phosphate appeared, indicating the presence of ATPase activity. The gels were photographed and total protein stained with Coomassie.

Testing for Free Cysteines. To determine the content of free cysteine thiol groups, the ABD-F labeling method in combination with SDS-PAGE and BSA as standard (*66*) was applied. For a control experiment with reduced disulfide bridges, 2 mM tributylphosphine was replaced by 5 mM tris-(2-carboxyethyl)phosphine (TCEP). After SDS-PAGE the gels were photographed using 366 nm UV light, stained with Coomassie, and rephotographed.

Analysis of Nucleotidase Reaction Products by RP-HPLC. For analysis of intermediates and products formed from prolonged ATP-hydrolysis, nucleotidase assays were performed as described above. Aliquots of 100 μL of reaction mixture were taken at the indicated time points, and the reaction was stopped with 30 μL of 0.5 M ice cold trichloroacetic acid. Samples were centrifuged for 2 min at 16 000*g* and the supernatant neutralized by addition to 40 μL of ice cold 0.5 M KOH. Until separation by RP-HPLC nucleotide samples were stored at −80 °C.

Adenosine nucleotides were separated as described (*15*) using a 15 cm × 2.0 mm, 3 μm/125 Å/C18 Aqua RP-HPLC column (Phenomenex, Torrance, CA) at a flow rate of 0.2 mL/min. Eluting nucleotides were detected and quantified by measuring the absorbance at 260 nm.

RESULTS

Cloning, Bacterial Expression, Refolding and Purification of NTPDase1−3 Extracellular Domains. The cDNA coding for the ectodomain of rat NTPDase1−3 was cloned into the bacterial expression vector pET45b(+) and expressed in ER2566 *E. coli* cells. All three constructs (for amino acid sequence see Figure S1 of the Supporting Information) showed a good overexpression of the recombinant protein. Because of overexpression and high content of disulfide bridges in the native protein, the NTPDase ectodomains precipitated entirely in the form of insoluble inclusion bodies in the *E. coli* cytosol (*67*). For high level production of the recombinant proteins, the cells were grown to high density using a fermenter in batch mode.

Table 1: Composition of Buffers and Incubation Temperature Used for Renaturation of NTPDase1−3 Ectodomains[a]

NTPDase1	NTPDase2	NTPDase3
0.6 M NACL	1.0 M L-arginine	1.0 M L-arginine
33 % (v/v) glycerol	20 % (v/v) glycerol	1.2 M NaCl
100 mM Tris-HCl	100 mM Tris-HCl	100 mM Tris-HCl
1 mM GSSG	1 mM GSSG	1 mM GSSG
2 mM GSH	2 mM GSH	2 mM GSH
pH 9.0	pH 9.0	pH 9.0
9−14 °C	4−9 °C	4−9 °C

[a] All buffers were sterile-filtered and thoroughly degassed. Refolding buffers further contained 1 mM EDTA, 1 mM benzamidine and 0.2 mM PMSF. Proteins were rapidly diluted 1:100 starting from 3 mg/mL protein in 6 M GdmCl, 5 mM HCl.

Solubilized and affinity-purified inclusion body proteins could be refolded to active enzyme by means of rapid dilution into nondenaturing buffers. No success was achieved with refolding by dialysis. Screening for the optimum refolding buffer was first done with incubation at 10 °C and included change of pH, variation of pH-buffer, and addition of varying amounts of different salts and folding helpers like L-arginine, glycerol, and sucrose. Refolding buffers all contained an oxido-shuffling system, of which the optimum composition was also determined. Furthermore, it was evaluated for NTPDase1, how initial and final protein and denaturant concentrations affected the specific and volumetric refolding yield. Success of renaturation was analyzed and compared by measurement of specific enzymatic activity.

The optimal composition of the refolding buffer was similar for all three enzymes with respect to pH and composition of the oxido-shuffling system (Table 1). Major differences existed in the dependence on the concentration of salt, l-arginine, and glycerol. Addition of known cofactors, substrates or products, such as Ca^{2+}, ATP, ADP, and AMP did not affect the refolding yield.

In the case of NTPDase1, the final denaturant concentrations had to be kept as low as possible (i.e., ≪30 mM, data not shown) to allow highest yields in protein folding. On the other hand, the initial concentration of GdmCl before dilution of the denatured protein to the refolding buffer had to be maintained at at least 5.5 M. It is likely that these high concentrations of denaturant are necessary to dissolve remaining secondary structure contacts that may lead to unproductive folding side reactions upon removal of denaturant. Together, this made a steep decrease of denaturant concentration by the use of a large dilution step desirable. However, the protein concentration before and after the dilution step affected the yield in such a way that a big dilution ratio would be disadvantageous: Not only had the final protein concentration to be kept at a minimum to favor first-order folding over higher order aggregation reactions but also had the protein concentration prior to the dilution step to remain low. Concentrating the denatured protein to more than 5 mg/mL resulted in dramatic losses in the subsequent refolding process. Therefore, as a compromise,

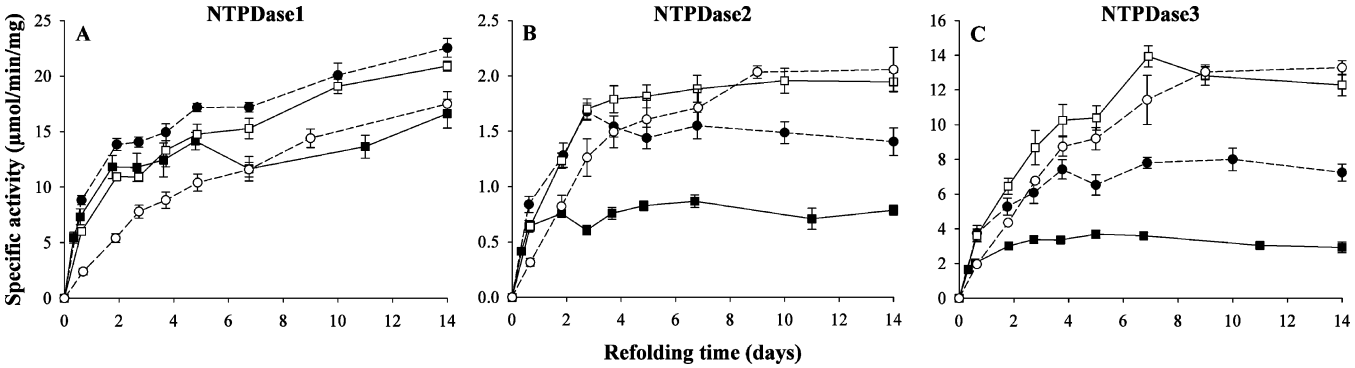

FIGURE 1: Refolding time course of His_6-tagged NTPDase ectodomains at different temperatures. Ni^{2+} affinity purified inclusion body protein was completely denatured and reduced as described in Experimental Procedures. Renaturation was initiated by rapid mixing of 15 μL of protein solution (3 mg/mL) into 1.5 mL of ice-cold refolding buffer. Batches were then incubated at the indicated temperatures (4 °C (○), 9 °C (□), 14 °C (●), 19 °C (■)) without stirring. Samples were withdrawn from at least five independent refolding batches at the given incubation time for immediate activity determination (200 μm ATP as substrate). Values are means ± SD.

the recombinant NTPDase ectodomains were diluted 1:100 from 3 mg/mL in 6 M GdmCl, 5 mM HCl into the specified refolding buffers.

The influence of temperature was then tested in the range from 4 °C to 19 °C (Figure 1). Higher temperatures (23 °C and 37 °C) resulted in almost no production of active protein. All proteins could be refolded at 9 °C with a slight tendency to lower temperatures for NTPDase2 and -3 and to higher temperatures for NTPDase1. For still unknown reasons, refolding kinetics are very slow, rendering the recombinant enzymes unsuitable for pulsed refolding (*67*).

Preliminary results on the refolding characteristics of enzyme variants give further evidence for the disulfide pattern previously suggested (*17*): two single cysteine knockout mutants C337A and C342A of NTPDase1 ectodomain and their combined knockout variant C337A/C342A could also be refolded to an active state with the combined knockout mutant attaining slightly more activity than the single mutants (data not shown). This indicates that the cysteine bridge C337−C342 stabilizes a loop formed by the surrounding residues that is not absolutely critical for nucleotidase activity.

After preparative refolding, the active enzyme was separated from wrongly folded, mainly aggregated protein. The same purification scheme consisting of a dialysis, an ion exchange, and a gel filtration step could be used for all three NTPDase variants and resulted in 95% pure, monomeric and monodisperse protein as judged from native PAGE (Figure 2), SDS-PAGE, size exclusion chromatography, and dynamic light scattering (data not shown). No free cysteine residues, which would indicate a partially unfolded protein, could be detected using the free sulfhydryl-specific ABD-F labeling reagent (Figure S2 of the Supporting Information). Bacterially expressed NTPDase ectodomains lack both transmembrane regions and are completely devoid of any N- or O-linked oligosaccharide chains. Their existence as monomers is hence in good agreement with earlier reports, which showed that oligomerization is mediated by the transmembrane regions in the case of NTPDase1 and -2 (*28*, *30*, *56*) and via side chain glycosylation in the case of NTPDase3 (*68*). Native PAGE and isoelectric focusing (not shown) indicated a slight microheterogeneity of the three enzyme preparations (Figure 2). Two or three closely migrating bands are visible. However, all separated protein bands belonging to one of the NTPDases displayed approximately the same specific activity in activity staining, ruling out the possibility of a contaminating fraction of unfolded protein. Full length expression of the three proteins could be verified by electrospray ionization mass spectrometry. The microheterogeneity observed is therefore likely due to modifications such as deamidation caused by the long refolding process at high pH. A detailed analysis at this point is not possible, because no high-resolution mass spectra could be obtained. Despite the slight microheterogeneity, crystallization trials were successful for the ectodomain of NTPDase2 (Figure S3 of the Supporting Information). This finding demonstrates the overall structural homogeneity of the protein sample with respect to folding and monodispersivity and the suitability for structural studies.

For maximal long-term stability and constant activity, the NTPDase variants were stored in 20 mM TrisHCl pH 7.5, 1 mM EDTA, 50 mM NaCl, 200 μg/mL BSA, 50% glycerol at −20 °C. This buffer was used for the calibration curves in all subsequent activity assays.

Substrate Specificity and Affinity. All three NTPDase ectodomains were able to hydrolyze a wide variety of tri- and diphosphonucleosides, including purine, pyrimidine, and 2′-deoxynucleotides (Table 2). Diphosphonucleosides are degraded at a lower rate than the corresponding triphosphonucleosides, and no activity toward the monophosphonucleoside AMP could be detected. The recombinant enzymes all show a slight reactivity toward pyrophosphate. This is not unexpected, as it is the simplest compound containing a phosphoanhydride bond and likely to bind to the catalytic site. Pyrophosphate was previously described as an inhibitor of NTPDases (*69*), a classification that may originate from it being a poor substrate.

For ATP and ADP, the substrates of the highest physiological importance, the apparent values of K_m and the maximal specific activity A_{max} were determined by measuring initial turnover velocities at different substrate concentrations (Figure 3, Table 4).

The bacterially expressed NTPDase1 variant showed almost maximum turnover at the lowest ADP concentration applicable to the malachite green assay (10 μM ADP, restriction to 1 μM phosphate release). First of all, this leads to a somewhat imprecise value for the K_m of ADP and to an underestimation of the error as calculated by the fitting algorithm. Second, this behavior complicates the determination of K_m for ATP that is apparently almost 2 orders of

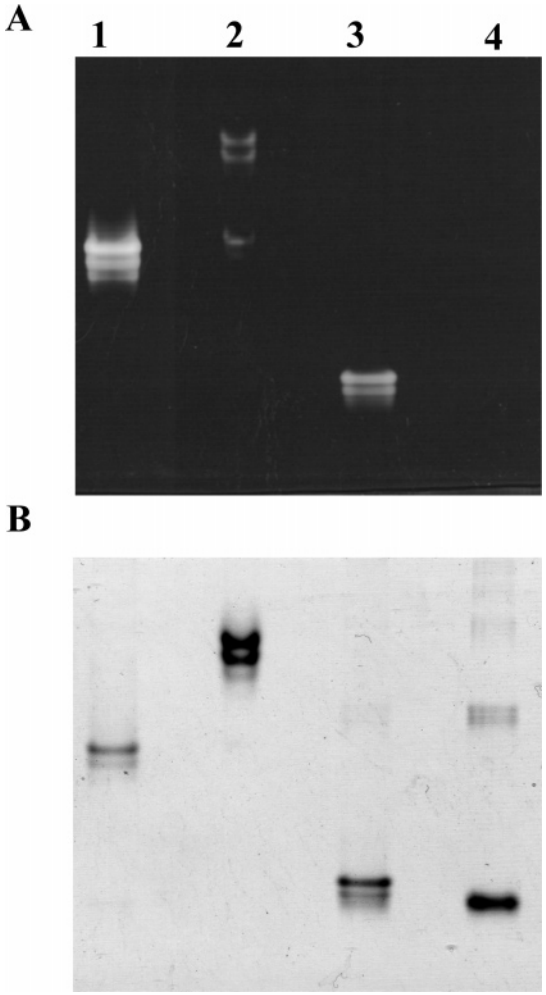

FIGURE 2: Native PAGE and activity staining. The refolded ectodomains of NTPDase1−3 and BSA were subjected to nondenaturing PAGE with a 10% resolving gel at pH 9.0. The stacking gel had a pH of 7.5. Lane 1: 3 μg of NTPDase1, lane 2: 6 μg of NTPDase2, lane 3: 3 μg of NTPDase3, lane 4: 3 μg of BSA. (A) After separation, the gel was stained for nucleotidase activity. White bands correspond to calcium phosphate deposition. The lowest band in lane 2 results from minor contamination with NTPDase1 during preparation of the gel (cross contamination). Since NTPDase1 is much more active than NTPDase2, the band is prominent in A but hardly visible in B. (B) The same gel as in A, Coomassie stained. Bands lost some of their sharpness during activity staining. Note that preparations of NTPDase1 and -3 contained BSA from the storage buffer. BSA is a largely monomeric protein with a molecular weight of 66 kDa and a calculated pI of 5.6.

magnitude larger. When 10% of substrate turnover from ATP is allowed, the released product of the first hydrolysis step, ADP, may to a substantial amount act as a competing substrate. To minimize this effect, we limited the phosphate release to 6 μM in all measurements and restricted the ATP concentrations to values where the initial ATPase velocity was bigger than ADPase turnover at 6 μm of released ADP (i.e., $\geq$ 60 μM ATP).

A direct comparison of the obtained kinetic data to previously published wild type data is difficult as values differ between species and the used reaction buffers vary in ionic strength and divalent cation concentrations. In addition, no K_m values of wild type rat NTPDases1−3 for ADP are available. However, the K_m values stated here are in the same range as those reported for several other cell surface NTPDases (*15*, *45 and references therein*). The maximal

Table 2: Substrate Specificity of NTPDase1−3 Refolded from Inclusion Bodies[a]

	relative activity (% ATP)		
substrate	NTPDase1	NTPDase2	NTPDase3
ATP	100.0 ± 8.6	100.0 ± 5.0	100.0 ± 6.7
GTP	79.0 ± 2.4	100.6 ± 9.8	173.1 ± 7.8
UTP	71.2 ± 4.0	79.3 ± 2.9	96.7 ± 3.5
CTP	100.2 ± 5.8	112.8 ± 3.3	82.0 ± 4.1
ITP	66.5 ± 8.2	98.1 ± 11.5	104.8 ± 10.3
dATP	106.3 ± 1.7	97.9 ± 3.9	75.6 ± 2.6
dTTP	106.4 ± 2.7	111.2 ± 5.8	93.1 ± 3.5
ADP	34.0 ± 0.1	44.3 ± 0.8	33.1 ± 0.8
UDP	44.3 ± 2.2	66.1 ± 7.0	19.5 ± 1.3
GDP	40.8 ± 2.3	73.6 ± 1.6	40.5 ± 2.8
PP_i	1.6 ± 0.7	10.4 ± 0.7	1.4 ± 0.5
AMP	not detectable	not detectable	not detectable

[a] Enzyme activity was assayed in reaction buffer with 500 μM $CaCl_2$ and 2 mM substrate. Reactions were started by addition of enzyme and P_i release measured as described in Experimental Procedures. Results are expressed as activity relative to ATP as the substrate and represent means ± SD from at least three independent experiments

specific ATPase and ADPase activities obtained here for the refolded NTPDase ectodomains are among the highest specific activities reported for purified enzyme preparations of mammalian cell surface NTPDases (*27*, *70*, *71*). The activity of the bacterially produced NTPDase1 ectodomain is even slightly higher than the highest reported value for secreted and affinity-purified NTPDase1 ectodomains (*28*, *47*, *56*). On the other hand, specific activities are substantially lower than reported for NTPDase5 and -6 produced by bacterial expression of the ectodomains and refolding (*16*, *55*). However, NTPDase5 and 6 together with NTPDase4 and -7 belong to a subclass of NTPDases (i.e., intracellular) that is distinct from the cell surface NTPDases as can be shown by phylogenetic analysis of multiple sequence alignment (*7*, *14*). Therefore, it is possible that the specific activities of these enzymes are higher or that the activity of the recombinantly expressed extracellular domains of NTPDase 5 and 6 is higher since they are not affected by the loss of two transmembrane helices and glycosylation.

The according k_{cat} values of the refolded ectodomains of NTPDase1−3 (Table 4) may be lower than the turnover rates of glycosylated and membrane-bound NTPDases as it was shown that NTPDase1, 2 and -8 ectodomains lose about 90% of their activity when expressed without transmembrane regions or when transmembrane interactions are dissolved by detergents (*30*, *56*, *57*). Wild type NTPDase3 loses 50% of activity upon deglycosylation with peptide *N*-glycosidase F (*22*, *68*).

Metal Cofactor Activation and Affinity. First attempts to refold the bacterially expressed NTPDase2 seemed to fail completely. No refolding buffer could be found, in which the specific activity became higher than 0.1 μmol min^{-1} mg^{-1}. It was realized later that this was not due to missing refolding success as such. Rather the assay buffer, that included $MgCl_2$ and $CaCl_2$, as used in wild type characterization (*6*, *26*, *45*) was not optimal for the recombinant soluble enzyme in terms of metal cofactor composition. While wild type NTPDase1 and -2 are equally activated by Mg^{2+} and Ca^{2+}, and NTPDase3 shows only little preference for the bigger Ca^{2+} ions (*14*, *15*, *26*), the bacterially expressed NTPDase ectodomains were apparently inhibited by the presence of $MgCl_2$ in the assay buffer. Therefore, we tested

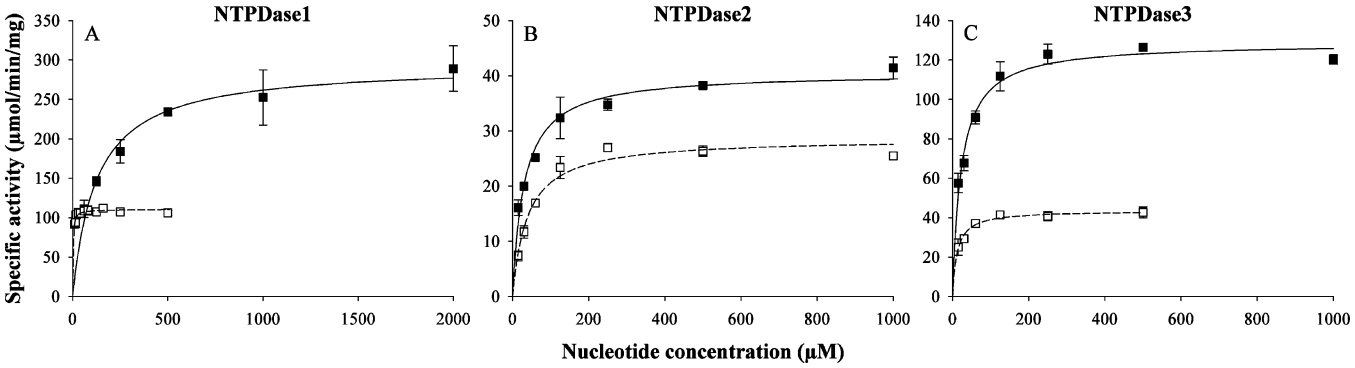

FIGURE 3: Linear Michaelis−Menten-Plot for the enzymatic turnover of ATP (■) and ADP (□) by recombinant NTPDase1−3. Data points are means ± SD from at least three independent experiments. Values for K_m and the maximal specific activity A_{max} (Table 4) were obtained using nonlinear regression to a hyperbolic saturation curve.

Table 3: Divalent Metal Ion Activation[a]

divalent metal ion	specific activity µmol P_i/(min mg) NTPDase1	NTPDase2	NTPDase3
Mg^{2+}	45.6 ± 2.2	9.9 ± 0.8	10.0 ± 0.4
Ca^{2+}	223.8 ± 3.0	42.6 ± 3.0	120.3 ± 3.0
Mn^{2+}	27.6 ± 2.5	9.4 ± 0.6	10.3 ± 0.9
Co^{2+}	113.7 ± 8.1	61.9 ± 7.8	20.3 ± 2.7
Ni^{2+}	37.8 ± 1.8	13.9 ± 1.3	29.1 ± 1.6
Cu^{2+}	26.4 ± 3.1	27.1 ± 2.5	42.4 ± 1.1
Zn^{2+}	245.2 ± 22.9	305.5 ± 6.2	72.1 ± 7.8
Sr^{2+}	198.6 ± 11.7	109.7 ± 11.1	182.6 ± 3.8
Cd^{2+}	105.3 ± 8.1	175.0 ± 6.1	48.9 ± 2.3
Ba^{2+}	7.0 ± 2.5	10.2 ± 1.1	29.0 ± 0.5
EDTA	0.1 ± 0.1	0.1 ± 0.1	-0.4 ± 0.5

[a] Enzyme activity was assayed in reaction buffer with 500 µM divalent metal chloride and 2 mM ATP. The concentration of EDTA introduced from protein storage buffer was 10 µM in all experiments. In a control experiment 500 µM EDTA was added to reaction buffer without divalent metal chloride. Reactions were started by addition of enzyme and P_i release measured as described in Experimental Procedures. Values are means ± SD from three independent experiments.

several divalent metal ions for their ability to activate the ATP hydrolysis of the purified NTPDase ectodomains.

Table 3 shows that Ca^{2+} ions indeed activate the NTPDase ectodomains much more than Mg^{2+} ions. In addition to Ca^{2+}, also Sr^{2+} and Zn^{2+} can activate all three NTPDase ectodomains to a high extent. NTPDase1 and -2 are further activated by Co^{2+} and Cd^{2+} ions.

Calcium activation was further analyzed by measuring ATP and ADP turnover at different total metal ion concentrations. Figure 4 shows that the calcium activation is saturable in both ATP and ADP hydrolysis. Effective concentrations of total calcium to achieve half-maximal activation (EC_{50}) have been calculated from a hyperbolic fit curve (Table 4). They are in the micromolar range with similar values for ATP and ADP as substrate. A comparable behavior with effective calcium concentrations of the same order of magnitude was shown for membrane-bound rat NTPDase3 expressed by CHO cells and human NTPDase1 ectodomain secreted by COS cells (*14*, *72*).

Dependence of ATPase and ADPase Activity on pH. Figure 5 (A−C) shows how ATPase and ADPase activities are affected by pH. The pH profiles are on the whole comparable to those of the membrane-bound human and mouse NTPDase1−3 (*15*). Dependence of wild type NTPDase2-mediated ADP hydrolysis on pH has not been reported so far.

The bacterially expressed NTPDase1 ectodomain has a neutral to alkaline pH optimum for both substrates. Refolded NTPDase2 ectodomain is active toward ATP at acidic to neutral pH and has a very narrow ADPase activity peak between pH 7.0 and 8.5. NTPDase3 hydrolyzes both substrates over a very broad pH range with ADPase activity increasing continuously from pH 4.5 to 10.

In Figure 5 (D) the ATPase:ADPase ratio is plotted against pH. As can clearly be seen, all three enzymes cleave ATP faster than ADP at any given pH. However, the ATPase:ADPase ratio is strongly depending on pH. Highest discrimination is found for all three enzymes at pH 5.5.

At physiological pH all three refolded NTPDase ectodomains reveal only negligible preference for ATP with almost the same value of about 2 for the ATPase:ADPase ratio. This is in contrast to wild type NTPDase2 and -3, which show a strong bias for ATP over ADP at physiological pH and only wild type NTPDase1 hydrolyzes both at approximately the same speed.

Product Formation Profiles. Large differences exist in the product formation course from prolonged ATP hydrolysis for wild type NTPDases. Wild type NTPDase1 apparently hydrolyzes ATP directly to AMP (*15*, *26*−*28*), whereas NTPDase2 and -3 release ADP. The accumulation of ADP is transient in the case of NTPDase3 but more sustained with NTPDase2 (*15*). Chen and Guidotti could show that the ability of NTPDase1 to retain ADP in the catalytic site depends on oligomerization via the transmembrane domains (*28*).

The recombinant NTPDase ectodomains described here lack both transmembrane domains and share the same low ATPase:ADPase ratio of around 2. All three enzymes would therefore be expected to transiently accumulate ADP. Figure 6 shows that this is indeed the case. However, the extracellular domain of NTPDase1 produces considerably less ADP as that of NTPDase2 and -3. It is likely that the higher specificity constant k_{cat}/K_m (Table 4) of NTPDase1 ectodomain for ADP alone is responsible, i.e., no mechanism to retain ADP in the active site exists. Rather, ADP is released from the catalytic site and then, as a better substrate, competes with ATP for rebinding.

Product formation profiles have been simulated by the program Dynafit (*73*, data not shown). On the basis of the k_{cat} and K_m values of the recombinant NTPDase1 ectodomain for ADP and ATP, not more than 5% ADP should ac-

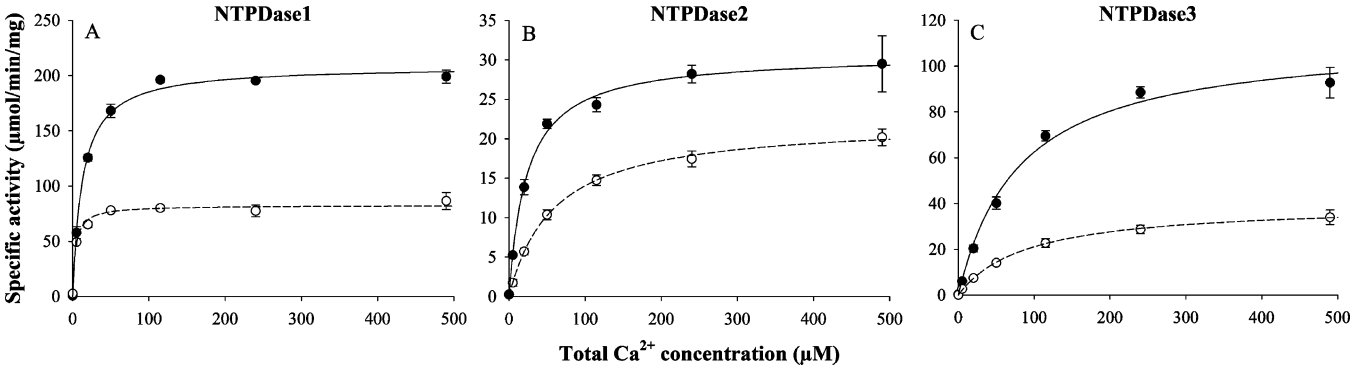

FIGURE 4: Calcium ion saturation curve for the enzymatic turnover of ATP (●) and ADP (○) by recombinant NTPDases. Total calcium concentration was corrected for the amount of EDTA (10 μM) introduced from the storage buffer. Data points are means ± SD from three independent experiments. The EC_{50} value for total calcium (Table 4) was calculated by nonlinear regression to a hyperbolic saturation curve.

Table 4: Physicochemical Properties of NTDPase1−3 Ectodomains Refolded from Inclusion Bodies[a]

property		NTPDase1	NTPDase2	NTPDase3
molecular weight (kDa)		52.0	50.6	52.0
ϵ_{spec} (280 nm, ox./red.) (L g^{-1} cm^{-1})		1.39/1.38	1.25/1.24	1.50/1.49
pI observed/calculated		6.3/6.2	7.2/7.0	5.5/5.8
optimum pH	ATP	7.5	6.0	6.5, 9.0
	ADP	8.5	7.5	9.0
K_m (μM)	ATP	125.0 ± 18.4	30.3 ± 3.0	22.6 ± 2.0
	ADP	1.9 ± 0.3	39.0 ± 4.0	11.8 ± 1.4
A_{max} (μmol min^{-1} mg^{-1})	ATP	294.5 ± 9.6	40.6 ± 0.9	128.7 ± 2.2
	ADP	110.6 ± 1.2	28.7 ± 0.7	43.6 ± 0.9
k_{cat} (s^{-1})	ATP	255.2 ± 8.3	34.3 ± 0.8	111.5 ± 1.9
	ADP	95.9 ± 1.0	24.2 ± 0.6	37.8 ± 0.8
k_{cat}/K_m (M^{-1} s^{-1})	ATP	2.0 × 10^6	1.1 × 10^6	4.9 × 10^6
	ADP	50.5 × 10^6	0.6 × 10^6	3.2 × 10^6
EC_{50} (total Ca^{2+}) (μM)	ATP	12.7 ± 0.7	23.5 ± 2.4	80.2 ± 7.4
	ADP	3.7 ± 0.5	58.5 ± 4.5	89.2 ± 8.3

[a] Molecular weights, specific extinction coefficients ϵ for completely oxidized/reduced disulfide bridges, and isoelectric points were calculated using the ProtParam Tool (*64*). Experimental pI values were obtained using the PhastSystem (Amersham Biosciences, Uppsala/Sweden). Enzyme activity was assayed in 50 mM TrisHCl, 100 mM NaCl, pH 7.4. For determination of K_m and the maximal specific activity A_{max} in ATP and ADP hydrolysis, the Ca^{2+} concentration was kept constant at 500 μM. Enzymes obeyed apparent Michaelis−Menten kinetics. Assuming 100% purity of the enzymes, k_{cat} was calculated from A_{max} by multiplication with the molecular weight of the enzymes. The EC_{50} value for total Ca^{2+} was determined for 500 μM substrate. Optimum pH was determined in a long-range pH buffer at constant ionic strength with 2 mM substrate and 500 μM $CaCl_2$. Reactions were started by addition of enzyme, and P_i release was measured as described in Experimental Procedures. Up to 10 μM EDTA was introduced from protein storage buffer to the reaction buffer. Values are means ± SE from at least three independent experiments.

cumulate at any time. Thus, the high specificity constant of recombinant NTPDase1 for ADP would match the product formation profiles of wild type NTPDase1. The discrepancy to the observed 30% intermediate ADP (Figure 6) concentration during ATP hydrolysis by recombinant NTPDase1 is unclear. In contrast, the accumulation of 50 to 60% ADP by recombinant NTPDase2 and -3 ectodomains is in good agreement with the kinetic parameters of these enzymes.

DISCUSSION

Cell surface NTPDases are key regulators in purinergic signaling. They are regarded as promising drug targets in anti-cancer and immune-disease therapy (*44*−*46*). On the other hand, administration of soluble forms of NTPDases seems to be effective in treatment of acute thrombotic disorders like stroke or myocardial infarction (*43*, *47*−*52*).

However, rapid screening of large compound libraries for subtype-selective NTPDase inhibitors will consume high amounts of active protein. Rational design of inhibitors and elucidation of the catalytic mechanism depends on the availability of a high-resolution X-ray crystal structure at least of the catalytic ectodomain. Screening for suitable crystallization conditions and growth of well diffracting crystals again needs concentrated protein of high quality. Even more highly pure protein, preferably produced at low costs, is required for use of NTPDases as pharmacotherapeutics, e.g., in antiplatelet therapy. The expression system described here will provide the protein that is suitable for all of the above-mentioned applications.

All three NTPDase ectodomains could be refolded to the active state by means of rapid dilution of denaturant-solubilized protein to nondenaturing buffers. Comparison of specific activities before and after separation of the active protein from wrongly folded protein (Figure 1 and 3) indicates that the refolding yield is between 5 and 15%. Although these numbers look disappointing at first, one has to consider that 10 cysteines have to be paired correctly and that the ectodomain is most probably composed of two structural domains. Therefore, the yield is acceptable and together with the strong overexpression of the proteins it allowed us to produce 15 mg of active NTPDase ectodomain per liter batch culture.

It can be reasoned from the high specific activities, wild type like pH profiles and the micromolar dissociation

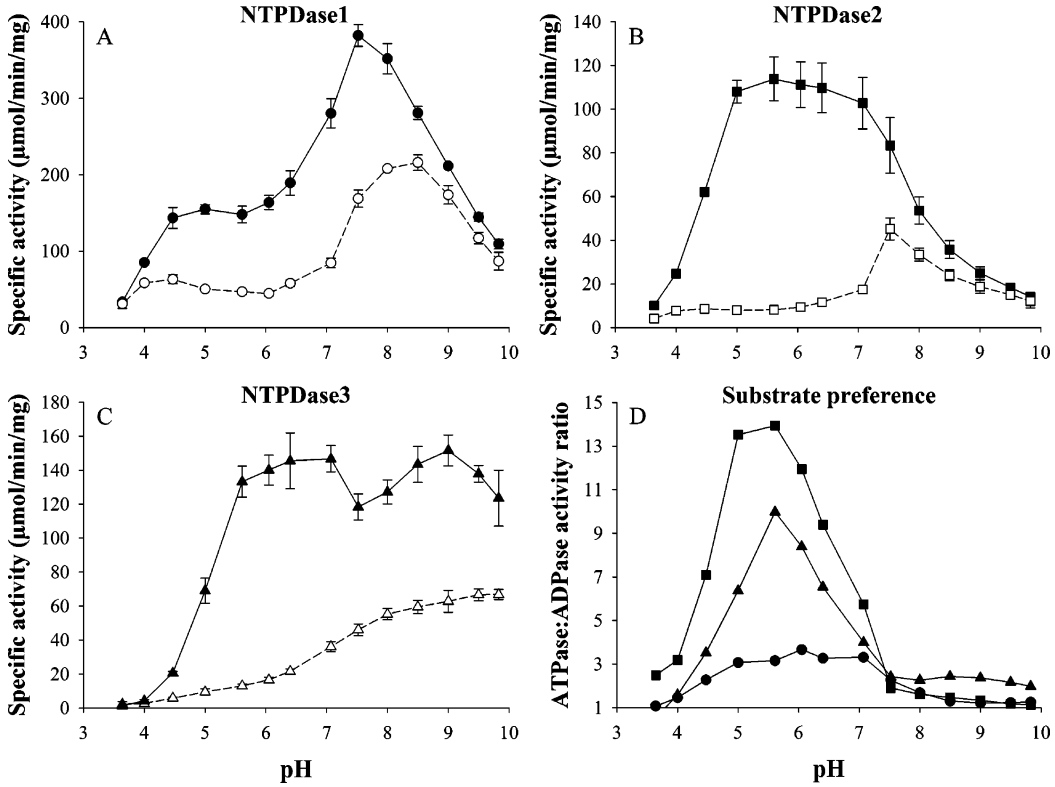

FIGURE 5: Influence of pH on NTPDase activity. (A−C) ATPase (closed symbols) and ADPase (open symbols) activity was assayed in the presence of 500 μM $CaCl_2$ and 2 mM substrate in a long-range pH buffer composed of 40 mM glycine, 40 mM acetic acid, 40 mM MOPS. The ionic strength was kept constant at 156 mM by supplementation with NaCl. (D) ATPase:ADPase ratio. Data was generated by dividing ATPase by ADPase activities. All three NTPDase ectodomains (NTPDase1 (●), NTPDase2 (■), NTPDase3 (▲)) hydrolyze ATP faster than ADP with the highest bias between pH 4.5 to 7.0 and NTPDase2 being the most discriminating diphosphohydrolase.

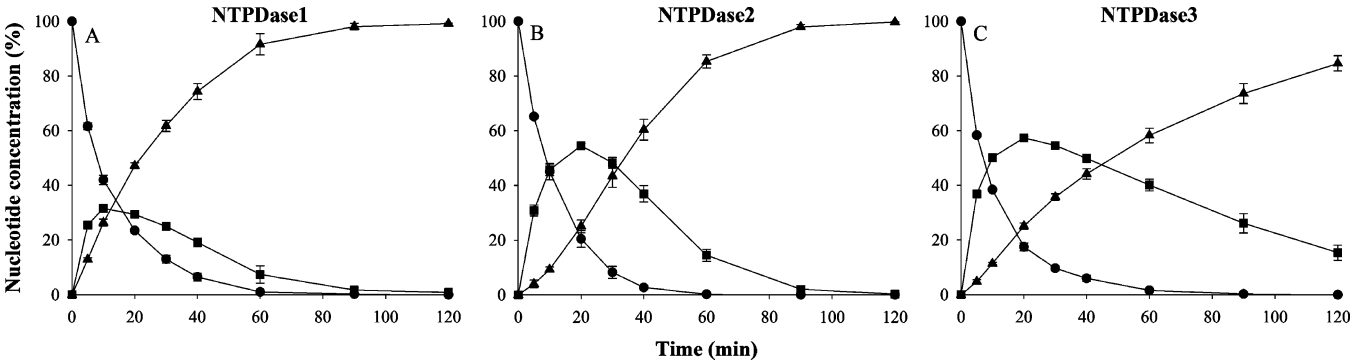

FIGURE 6: Product formation profiles of recombinant NTPDases. ATP hydrolysis was initiated by addition of enzyme to reaction buffer containing 500 μM ATP and 500 μM $CaCl_2$. The enzyme concentration was 250 ng/mL (NTPDase1), 1000 ng/mL (NTPDase2), and 450 ng/mL (NTPDase3). Aliquots (100 μL) were taken at the indicated time points and the reaction stopped by addition of 30 μL of 0.5 M TCA. Nucleotides (ATP (●), ADP (■), AMP (▲)) were separated using RP-HPLC. Symbols represent means ± SD from three independent experiments.

constants for substrates and calcium that the active site of the bacterially expressed NTPDase ectodomains is intact. NTPDase ectodomains produced at milligram scale with the described method should therefore allow successful identification of specific inhibitors in high throughput screening (*45*, *74*), that will also be effective *in vivo*. In addition, the presented expression system constitutes an easy method to further characterize NTPDases by determining the influence of mutations on folding and activity.

The minor differences to wild type enzymatic properties, such as change in ATPase:ADPase ratio at physiological pH, different metal cofactor specificity and altered product formation course (especially NTPDase1) can be attributed to the concomitant lack of transmembrane regions and side chain glycosylation (*22*, *28*, *30*, *75*, *76*).

It had been shown before for NTPDase1 and -2 that the absence of the transmembrane helices results in altered ATPase:ADPase ratios that are almost equal to the values reported here (*30*, *76*). The closely related human NTPDase8 does also show a decreased ATPase:ADPase ratio when only the extracellular domain is expressed. Furthermore, the NTPDase8 ectodomain is much more strongly activated by Ca^{2+} than by Mg^{2+} just as the variants described here (*57*). To our knowledge no previous reports about eukaryotic expression of NTPDase3 without transmembrane domains exist. However, the knockout of the conserved glycosylation

site N81 in human NTPDase3 reduced the ATPase:ADPase ratio similarly. The mutations in the glycosylation site made the enzyme also more specific for Ca^{2+} as a cofactor (*22*, *25*, *68*).

Missing transmembrane interactions and lack of side chain glycosylation due to the bacterial expression do not only explain the change in ATPase:ADPase ratios and the increased Ca^{2+} preference of the enzymes but also the altered product formation courses. As a direct consequence of the strongly reduced ATPase:ADPase ratio of NTPDase2 ectodomain, the accumulation of ADP upon prolonged ATP hydrolysis is becoming more transient, closer to the behavior reported for wild type NTPDase3. The release of ADP by the bacterially expressed NTPDase1 ectodomain is most likely due to the missing transmembrane interaction as was shown before (*28*).

The absence of N-linked glycosylation could be expected to result in less soluble and much more aggregation-prone proteins. However, the recombinant ectodomains could be concentrated to several mg/mL without loss of monodispersity as determined by dynamic light scattering. As glycan side chains are a cause for microheterogeneity and often interfere with protein crystallization, the bacterially expressed ectodomains will not only be more amenable for crystallization than membrane-bound or detergent-solubilized NTPDases but probably also crystallize more readily than glycosylated ectodomains secreted from mammalian or yeast expression systems. A first success could be achieved with crystallization of the NTPDase2 ectodomain (Figure S3 of the Supporting Information).

In 1998 a soluble variant of human CD39 (NTPDase1) was first proposed for application as antithrombotic agent (*47*). The ideal ATPase administered in antiplatelet therapy should have a very high catalytic efficiency and preferably hydrolyze extracellular ATP directly to AMP without significant accumulation of the platelet activator ADP. This is indeed the case for membrane-bound wild type NTPDase1 because a mechanism exists, that prevents dissociation of ADP from the catalytic site before hydrolysis to AMP proceeds. Soluble NTPDase1 ectodomains lack this mechanism that depends on transmembrane domain interactions and oligomerization (*26*, *28*).

The bacterially expressed NTPDase1 ectodomain does also release ADP in prolonged hydrolysis of 500 μM ATP (Figure 6 A). However, the peak concentration of ADP is only half of that seen with the other two NTPDase ectodomains (Figure 6 B, C). In contrast to the membrane-bound NTPDase1, only the very high ratio in catalytic efficiencies for ADP and ATP is responsible. Considering that physiological concentrations of extracellular ATP are unlikely to exceed 10 μM (*2*), one can assume that no substantial accumulation of the platelet activator ADP would occur in case of NTPDase1 ectodomain administration. Thus, the higher specificity for ADP in combination with the high overall specific activity of the enzyme would make the bacterially expressed NTPDase1 ectodomain an ideal antithrombotic agent. Furthermore bacterial expression allows production of the protein at low costs and avoids viral contamination. Potential exists, that the site-directed mutations H59G and S57A will further improve the catalytic efficiency for ADP. These substitutions increased the ADPase activity of soluble NTPDase1 secreted from COS cells while leaving the ATPase activity unaltered (*75*, *76*). It is also possible that variants can be developed which maintain the absence of ADP release despite of missing side chain glycosylation and oligomerization.

To avoid immunogenicity upon repeated clinical application, one would try to use the human form of NTPDase1 ectodomain refolded from inclusion bodies as therapeutic agent. The high degree of sequence identity between rat and human NTPDase1 of 74% (93% similarity) in the ectodomain suggests that the human NTPDase1 ectodomain produced with the described method will have similar catalytic efficiencies for ADP and ATP.

In conclusion, the recombinant overexpression of the three rat NTPDases yielded active enzymes, whose catalytic properties are overall in agreement with those of the wild type enzymes, taking into account the modulation of enzyme activity by the transmembrane helices and by glycosylation. Therefore, the recombinant enzymes will not only facilitate structural studies but also the design of specific inhibitors and the production of enzyme as a protein drug in antiplatelet therapy.

ACKNOWLEDGMENT

The authors thank Prof. Herbert Zimmermann for kindly providing full length clones of rat NTPDase1−3. We also acknowledge Katharina Schutt, José Muñoz, Manuela Rösler, Anja Kuhnert, and Katrin Jungmann for their technical assistance.

SUPPORTING INFORMATION AVAILABLE

Amino acid sequences of the NTPDase constructs resulting from ABD-F labeling of free cysteines and a figure of an NTPDase2 crystal. This material is available free of charge via the Internet at http://pubs.acs.org.

REFERENCES

1. Yegutkin, G. G., and Burnstock, G. (2000) Inhibitory effects of some purinergic agents on ecto-ATPase activity and pattern of stepwise ATP hydrolysis in rat liver plasma membranes, *Biochim. Biophys. Acta 1466*, 234−244.
2. Schwiebert, E. M. (2001) ATP release mechanisms, ATP receptors and purinergic signalling along the nephron, *Clin. Exp. Pharmacol. Physiol 28*, 340−350.
3. Schwiebert, E. M., and Zsembery, A. (2003) Extracellular ATP as a signaling molecule for epithelial cells, *Biochim. Biophys. Acta 1615*, 7−32.
4. Zimmermann, H. (2000) Extracellular metabolism of ATP and other nucleotides, *Naunyn-Schmiedebergs Arch. Pharmacol. 362*, 299−309.
5. Zimmermann, H. (2001) Ectonucleotidases: Some recent developments and a note on nomenclature, *Drug Dev. Res. 52*, 44−56.
6. Failer, B. U., Aschrafi, A., Schmalzing, G., and Zimmermann, H. (2003) Determination of native oligomeric state and substrate specificity of rat NTPDase1 and NTPDase2 after heterologous expression in Xenopus oocytes, *Eur. J. Biochem. 270*, 1802−1809.
7. Robson, S. C., Sévigny, J., and Zimmerman, H. (2006) The E-NTPDase family of ectonucleotidases: Structure function relationships and pathophysiological significance, *Purinergic Signal. 2*, 409−430.
8. Knöfel, T., and Sträter, N. (1999) X-ray structure of the Escherichia coli periplasmic 5′-nucleotidase containing a dimetal catalytic site, *Nat. Struct. Biol. 6*, 448−453.
9. Sträter, N. (2006) Ecto-5′-nucleotidase: Structure function relationships, *Purinergic Signal. 2*, 343−350.
10. Trombetta, E. S., and Helenius, A. (1999) Glycoprotein reglucosylation and nucleotide sugar utilization in the secretory pathway: identification of a nucleoside diphosphatase in the endoplasmic reticulum, *EMBO J. 18*, 3282−3292.

11. Braun, N., Fengler, S., Ebeling, C., Servos, J., and Zimmermann, H. (2000) Sequencing, functional expression and characterization of rat NTPDase6, a nucleoside diphosphatase and novel member of the ecto-nucleoside triphosphate diphosphohydrolase family, *Biochem. J. 351 Pt 3*, 639−647.
12. Shi, J. D., Kukar, T., Wang, C. Y., Li, Q. Z., Cruz, P. E., Davoodi-Semiromi, A., Yang, P., Gu, Y., Lian, W., Wu, D. H., and She, J. X. (2001) Molecular cloning and characterization of a novel mammalian endo-apyrase (LALP1), *J. Biol. Chem. 276*, 17474−17478.
13. Bigonnesse, F., Levesque, S. A., Kukulski, F., Lecka, J., Robson, S. C., Fernandes, M. J., and Sévigny, J. (2004) Cloning and characterization of mouse nucleoside triphosphate diphosphohydrolase-8, *Biochemistry 43*, 5511−5519.
14. Vorhoff, T., Zimmermann, H., Pelletier, J., Sévigny, J., and Braun, N. (2005) Cloning and characterization of the ecto-nucleotidase NTPDase3 from rat brain: Predicted secondary structure and relation to other members of the E-NTPDase family and actin, *Purinergic Signal. 1*, 259−270.
15. Kukulski, F., Lévesque, S. A., Lavoie, É. G., Lecka, J., Bigonnesse, F., Knowles, A. F., Robson, S. C., Kirley, T. L., and Sévigny, J. (2005) Comparative hydrolysis of P2 receptor agonists by NTPDases 1, 2, 3 and 8, *Purinergic Signal. 1*, 193−204.
16. Ivanenkov, V. V., Murphy-Piedmonte, D. M., and Kirley, T. L. (2003) Bacterial expression, characterization, and disulfide bond determination of soluble human NTPDase6 (CD39L2) nucleotidase: implications for structure and function, *Biochemistry 42*, 11726−11735.
17. Ivanenkov, V. V., Meller, J., and Kirley, T. L. (2005) Characterization of disulfide bonds in human nucleoside triphosphate diphosphohydrolase 3 (NTPDase3): implications for NTPDase structural modeling, *Biochemistry 44*, 8998−9012.
18. Christoforidis, S., Papamarcaki, T., and Tsolas, O. (1996) Human placental ATP diphosphohydrolase is a highly N-glycosylated plasma membrane enzyme, *Biochim. Biophys. Acta 1282*, 257−262.
19. Lewis-Carl, S., and Kirley, T. L. (1997) Immunolocalization of the ecto-ATPase and ecto-apyrase in chicken gizzard and stomach. Purification and N-terminal sequence of the stomach ecto-apyrase, *J. Biol. Chem. 272*, 23645−23652.
20. Sévigny, J., Levesque, F. P., Grondin, G., and Beaudoin, A. R. (1997) Purification of the blood vessel ATP diphosphohydrolase, identification and localisation by immunological techniques, *Biochim. Biophys. Acta 1334*, 73−88.
21. Kansas, G. S., Wood, G. S., and Tedder, T. F. (1991) Expression, distribution, and biochemistry of human CD39. Role in activation-associated homotypic adhesion of lymphocytes, *J. Immunol. 146*, 2235−2244.
22. Murphy, D. M., and Kirley, T. L. (2003) Asparagine 81, an invariant glycosylation site near apyrase conserved region 1, is essential for full enzymatic activity of ecto-nucleoside triphosphate diphosphohydrolase 3, *Arch. Biochem. Biophys. 413*, 107−115.
23. Handa, M., and Guidotti, G. (1996) Purification and cloning of a soluble ATP-diphosphohydrolase (apyrase) from potato tubers (Solanum tuberosum), *Biochem. Biophys. Res. Commun. 218*, 916−923.
24. Smith, T. M., and Kirley, T. L. (1999) Site-directed mutagenesis of a human brain ecto-apyrase: evidence that the E-type ATPases are related to the actin/heat shock 70/sugar kinase superfamily, *Biochemistry 38*, 321−328.
25. Kirley, T. L., Crawford, P. A., and Smith, T. M. (2006) The structure of the nucleoside triphosphate diphosphohydrolases (NTPDases) as revealed by mutagenic and computational modeling analyses, *Purinergic Signal. 2*, 379−389.
26. Heine, P., Braun, N., Heilbronn, A., and Zimmermann, H. (1999) Functional characterization of rat ecto-ATPase and ecto-ATP diphosphohydrolase after heterologous expression in CHO cells, *Eur. J. Biochem. 262*, 102−107.
27. Kukulski, F., and Komoszynski, M. (2003) Purification and characterization of NTPDase1 (ecto-apyrase) and NTPDase2 (ecto-ATPase) from porcine brain cortex synaptosomes, *Eur. J. Biochem. 270*, 3447−3454.
28. Chen, W., and Guidotti, G. (2001) Soluble apyrases release ADP during ATP hydrolysis, *Biochem. Biophys. Res. Commun. 282*, 90−95.
29. Wink, M. R., Braganhol, E., Tamajusuku, A. S., Lenz, G., Zerbini, L. F., Libermann, T. A., Sévigny, J., Battastini, A. M., and Robson, S. C. (2006) Nucleoside triphosphate diphosphohydrolase-2 (NTPDase2/CD39L1) is the dominant ectonucleotidase expressed by rat astrocytes, *Neuroscience 138*, 421−432.
30. Grinthal, A., and Guidotti, G. (2002) Transmembrane domains confer different substrate specificities and adenosine diphosphate hydrolysis mechanisms on CD39, CD39L1, and chimeras, *Biochemistry 41*, 1947−1956.
31. Mateo, J., Harden, T. K., and Boyer, J. L. (1999) Functional expression of a cDNA encoding a human ecto-ATPase, *Br. J. Pharmacol. 128*, 396−402.
32. Fausther, M., Lecka, J., Kukulski, F., Lévesque, S. A., Pelletier, J., Zimmermann, H., Dranoff, J. A., and Sévigny, J. (2007) Cloning, purification, and identification of the liver canalicular ecto-ATPase as NTPDase8, *Am. J. Physiol. Gastrointest. Liver Physiol. 292*, G785−G795.
33. Smith, T. M., and Kirley, T. L. (1998) Cloning, sequencing, and expression of a human brain ecto-apyrase related to both the ecto-ATPases and CD39 ecto-apyrases, *Biochim. Biophys. Acta 1386*, 65−78.
34. Kaczmarek, E., Koziak, K., Sévigny, J., Siegel, J. B., Anrather, J., Beaudoin, A. R., Bach, F. H., and Robson, S. C. (1996) Identification and characterization of CD39/vascular ATP diphosphohydrolase, *J. Biol. Chem. 271*, 33116−33122.
35. Marcus, A. J., Broekman, M. J., Drosopoulos, J. H., Islam, N., Alyonycheva, T. N., Safier, L. B., Hajjar, K. A., Posnett, D. N., Schoenborn, M. A., Schooley, K. A., Gayle, R. B., and Maliszewski, C. R. (1997) The endothelial cell ecto-ADPase responsible for inhibition of platelet function is CD39, *J. Clin. Invest. 99*, 1351−1360.
36. Enjyoji, K., Sévigny, J., Lin, Y., Frenette, P. S., Christie, P. D., Esch, J. S., II, Imai, M., Edelberg, J. M., Rayburn, H., Lech, M., Beeler, D. L., Csizmadia, E., Wagner, D. D., Robson, S. C., and Rosenberg, R. D. (1999) Targeted disruption of cd39/ATP diphosphohydrolase results in disordered hemostasis and thromboregulation, *Nat. Med. 5*, 1010−1017.
37. Mizumoto, N., Kumamoto, T., Robson, S. C., Sévigny, J., Matsue, H., Enjyoji, K., and Takashima, A. (2002) CD39 is the dominant Langerhans cell-associated ecto-NTPDase: modulatory roles in inflammation and immune responsiveness, *Nat. Med. 8*, 358−365.
38. Robson, S. C., Enjyoji, K., Goepfert, C., Imai, M., Kaczmarek, E., Lin, Y., Sévigny, J., and Warny, M. (2001) Modulation of extracellular nucleotide-mediated signaling by CD39/nucleoside triphosphate diphosphohydrolase-1, *Drug Dev. Res. 53*, 193−207.
39. Robson, S. C., Kaczmarek, E., Siegel, J. B., Candinas, D., Koziak, K., Millan, M., Hancock, W. W., and Bach, F. H. (1997) Loss of ATP diphosphohydrolase activity with endothelial cell activation, *J. Exp. Med. 185*, 153−163.
40. Dzhandzhugazyan, K. N., Kirkin, A. F., thor Straten, P., and Zeuthen, J. (1998) Ecto-ATP diphosphohydrolase/CD39 is overexpressed in differentiated human melanomas, *FEBS Lett. 430*, 227−230.
41. Kittel, A., Garrido, M., and Varga, G. (2002) Localization of NTPDase1/CD39 in normal and transformed human pancreas, *J. Histochem. Cytochem. 50*, 549−556.
42. Buffon, A., Ribeiro, V. B., Wink, M. R., Casali, E. A., and Sarkis, J. J. (2007) Nucleotide metabolizing ecto-enzymes in Walker 256 tumor cells: molecular identification, kinetic characterization and biochemical properties, *Life Sci. 80*, 950−958.
43. Marcus, A. J., Broekman, M. J., Drosopoulos, J. H., Islam, N., Pinsky, D. J., Sesti, C., and Levi, R. (2003) Heterologous cell-cell interactions: thromboregulation, cerebroprotection and cardioprotection by CD39 (NTPDase-1), *J. Thromb. Haemost. 1*, 2497−2509.
44. Gendron, F. P., Benrezzak, O., Krugh, B. W., Kong, Q., Weisman, G. A., and Beaudoin, A. R. (2002) Purine signaling and potential new therapeutic approach: possible outcomes of NTPDase inhibition, *Curr. Drug Targets 3*, 229−245.
45. Iqbal, J., Vollmayer, P., Braun, N., Zimmermann, H., and Müller, C. E. (2005) A capillary electrophoresis method for the characterization of ecto-nucleoside triphosphate diphosphohydrolases (NTPDases) and the analysis of inhibitors by in-capillary enzymatic microreaction, *Purinergic Signal. 1*, 349−358.
46. Müller, C. E., Iqbal, J., Baqi, Y., Zimmermann, H., Rollich, A., and Stephan, H. (2006) Polyoxometalates−a new class of potent ecto-nucleoside triphosphate diphosphohydrolase (NTPDase) inhibitors, *Bioorg. Med. Chem. Lett. 16*, 5943−5947.
47. Gayle, R. B., 3., Maliszewski, C. R., Gimpel, S. D., Schoenborn, M. A., Caspary, R. G., Richards, C., Brasel, K., Price, V.,

Drosopoulos, J. H., Islam, N., Alyonycheva, T. N., Broekman, M. J., and Marcus, A. J. (1998) Inhibition of platelet function by recombinant soluble ecto-ADPase/CD39, *J. Clin. Invest. 101*, 1851−1859.

48. Pinsky, D. J., Broekman, M. J., Peschon, J. J., Stocking, K. L., Fujita, T., Ramasamy, R., Connolly, E. S., Jr., Huang, J., Kiss, S., Zhang, Y., Choudhri, T. F., McTaggart, R. A., Liao, H., Drosopoulos, J. H., Price, V. L., Marcus, A. J., and Maliszewski, C. R. (2002) Elucidation of the thromboregulatory role of CD39/ectoapyrase in the ischemic brain, *J. Clin. Invest. 109*, 1031−1040.
49. Marcus, A. J., Broekman, M. J., Drosopoulos, J. H., Islam, N., Pinsky, D. J., Sesti, C., and Levi, R. (2003) Metabolic control of excessive extracellular nucleotide accumulation by CD39/ecto-nucleotidase-1: implications for ischemic vascular diseases, *J. Pharmacol. Exp. Ther. 305*, 9−16.
50. Belayev, L., Khoutorova, L., Deisher, T. A., Belayev, A., Busto, R., Zhang, Y., Zhao, W., and Ginsberg, M. D. (2003) Neuroprotective effect of SolCD39, a novel platelet aggregation inhibitor, on transient middle cerebral artery occlusion in rats, *Stroke 34*, 758−763.
51. Buergler, J. M., Maliszewski, C. R., Broekman, M. J., Kaluza, G. L., Schulz, D. G., Marcus, A. J., Raizner, A. E., Kleiman, N. S., and Ali, N. M. (2005) Effects of SolCD39, a novel inhibitor of Platelet Aggregation, on Platelet Deposition and Aggregation after PTCA in a Porcine Model, *J. Thromb. Thrombolysis 19*, 115−122.
52. Haller, C. A., Cui, W., Wen, J., Robson, S. C., and Chaikof, E. L. (2006) Reconstitution of CD39 in liposomes amplifies nucleoside triphosphate diphosphohydrolase activity and restores thromboregulatory properties, *J. Vasc. Surg. 43*, 816−823.
53. Darling, A. (2002) Validation of biopharmaceutical purification processes for virus clearance evaluation, *Mol. Biotechnol. 21*, 57−83.
54. Werz, W., Hoffmann, H., Haberer, K., and Walter, J. K. (1997) Strategies to avoid virus transmissions by biopharmaceutic products, *Arch. Virol. Suppl. 13*, 245−256.
55. Murphy-Piedmonte, D. M., Crawford, P. A., and Kirley, T. L. (2005) Bacterial expression, folding, purification and characterization of soluble NTPDase5 (CD39L4) ecto-nucleotidase, *Biochim. Biophys. Acta 1747*, 251−259.
56. Wang, T. F., Ou, Y., and Guidotti, G. (1998) The transmembrane domains of ectoapyrase (CD39) affect its enzymatic activity and quaternary structure, *J. Biol. Chem. 273*, 24814−24821.
57. Knowles, A. F., and Li, C. (2006) Molecular cloning and characterization of expressed human ecto-nucleoside triphosphate diphosphohydrolase 8 (E-NTPDase 8) and its soluble extracellular domain, *Biochemistry 45*, 7323−7333.
58. Kegel, B., Braun, N., Heine, P., Maliszewski, C. R., and Zimmermann, H. (1997) An ecto-ATPase and an ecto-ATP diphosphohydrolase are expressed in rat brain, *Neuropharmacology 36*, 1189−1200.
59. Lu, Q., Porter, L. D., Cui, X., and Sanborn, B. M. (2001) Ecto-ATPase mRNA is regulated by FSH in Sertoli cells, *J. Androl. 22*, 289−301.
60. Notredame, C., Higgins, D. G., and Heringa, J. (2000) T-Coffee: A novel method for fast and accurate multiple sequence alignment, *J. Mol. Biol. 302*, 205−217.
61. Cuff, J. A., Clamp, M. E., Siddiqui, A. S., Finlay, M., and Barton, G. J. (1998) JPred: a consensus secondary structure prediction server, *Bioinformatics 14*, 892−893.
62. Horn, U., Strittmatter, W., Krebber, A., Knüpfer, U., Kujau, M., Wenderoth, R., Müller, K., Matzku, S., Plückthun, A., and Riesenberg, D. (1996) High volumetric yields of functional dimeric miniantibodies in Escherichia coli, using an optimized expression vector and high-cell-density fermentation under non-limited growth conditions, *Appl. Microbiol. Biotechnol. 46*, 524−532.
63. Rudolph, R., Böhm, G., Lilie, H., and Jaenicke, R. (1997) Folding proteins, in *Protein Function: A Practical Approach* pp 57−99, (Hg. T. E. Creighton) Oxford University Press, Oxford.
64. Gasteiger, E., Gattiker, A., Hoogland, C., Ivanyi, I., Appel, R. D., and Bairoch, A. (2003) ExPASy: The proteomics server for in-depth protein knowledge and analysis, *Nucleic Acids Res. 31*, 3784−3788.
65. Baykov, A. A., Evtushenko, O. A., and Avaeva, S. M. (1988) A malachite green procedure for orthophosphate determination and its use in alkaline phosphatase-based enzyme immunoassay, *Anal. Biochem. 171*, 266−270.
66. Kirley, T. L. (1989) Reduction and fluorescent labeling of cyst(e)ine-containing proteins for subsequent structural analyses, *Anal. Biochem. 180*, 231−236.
67. Lilie, H., Schwarz, E., and Rudolph, R. (1998) Advances in refolding of proteins produced in E. coli, *Curr. Opin. Biotechnol. 9*, 497−501.
68. Smith, T. M., and Kirley, T. L. (1999) Glycosylation is essential for functional expression of a human brain ecto-apyrase, *Biochemistry 38*, 1509−1516.
69. Knowles, A. F., Nagy, A. K., Strobel, R. S., and Wu-Weis, M. (2002) Purification, characterization, cloning, and expression of the chicken liver ecto-ATP-diphosphohydrolase, *Eur. J. Biochem. 269*, 2373−2382.
70. Moodie, F. D., Baum, H., Butterworth, P. J., and Peters, T. J. (1991) Purification and characterisation of bovine spleen ADPase, *Eur. J. Biochem. 202*, 1209−1215.
71. Sévigny, J., Cote, Y. P., and Beaudoin, A. R. (1995) Purification of pancreas type-I ATP diphosphohydrolase and identification by affinity labelling with the 5′-p-fluorosulphonylbenzoyladenosine ATP analogue, *Biochem. J. 312* (*Pt 2*), 351−356.
72. Drosopoulos, J. H. (2002) Roles of Asp54 and Asp213 in Ca2+ utilization by soluble human CD39/ecto-nucleotidase, *Arch. Biochem. Biophys. 406*, 85−95.
73. Kuzmic, P. (1996) Program DYNAFIT for the analysis of enzyme kinetic data: application to HIV proteinase, *Anal. Biochem. 237*, 260−273.
74. Windsor, J. B., Thomas, C., Hurley, L., Roux, S. J., and Lloyd, A. M. (2002) Automated colorimetric screen for apyrase inhibitors, *Biotechniques 33*, 1024−1030.
75. Drosopoulos, J. H., Broekman, M. J., Islam, N., Maliszewski, C. R., Gayle, R. B., III, and Marcus, A. J. (2000) Site-directed mutagenesis of human endothelial cell ecto-ADPase/soluble CD39: requirement of glutamate 174 and serine 218 for enzyme activity and inhibition of platelet recruitment, *Biochemistry 39*, 6936−6943.
76. Grinthal, A., and Guidotti, G. (2000) Substitution of His59 converts CD39 apyrase into an ADPase in a quaternary structure dependent manner, *Biochemistry 39*, 9−16.

BI701103Y